ARTICLE
Journal of Cellular Biochemistry 116:2870–2881 (2015)

Journal of Cellular Biochemistry

MicroRNA-155 Regulates ROS Production, NO Generation, Apoptosis and Multiple Functions of Human Brain Microvessel Endothelial Cells Under Physiological and Pathological Conditions

Yajing Liu,[1] Qunwen Pan,[1] Yuhui Zhao,[2] Caixia He,[1] Kexia Bi,[1] Yusen Chen,[1] Bin Zhao,[1] Yanfang Chen,[1,2*] and Xiaotang Ma[1*]

[1]*Guangdong Key Laboratory of Age-Related Cardiac and Cerebral Diseases, Institute of Neurology, Affiliated Hospital of Guangdong Medical College, Zhanjiang 524001, China*

[2]*Department of Pharmacology and Toxicology, Boonshoft School of Medicine, Wright State University, Dayton, Ohio 45435*

ABSTRACT

The microRNA-155 (miR155) regulates various functions of cells. Dysfunction or injury of endothelial cells (ECs) plays an important role in the pathogenesis of various vascular diseases. In this study, we investigated the role and potential mechanisms of miR155 in human brain microvessel endothelial cells (HBMECs) under physiological and pathological conditions. We detected the effects of miR155 silencing on ROS production, NO generation, apoptosis and functions of HBMECs at basal and in response to oxidized low density lipoprotein (ox-LDL). Western blot and q-PCR were used for analyzing the gene expression of epidermal growth factor receptor (EGFR)/extracellular regulated protein kinases (ERK)/p38 mitogen-activated protein kinase (p38 MAPK), phosphatidylinositol-3-kinase (PI3K) and serine/threonine kinase(Akt), activated caspase-3, and intercellular adhesion molecule-1 (ICAM-1). Results showed that under both basal and challenge situations: (1) Silencing of miR155 decreased apoptosis and reactive oxygen species (ROS) production of HBMECs, whereas, promoted nitric oxide (NO) generation. (2) Silencing of miR155 increased the proliferation, migration, and tube formation ability of HBMECs, while decreased cell adhesion ability. (3) Gene expression analyses showed that EGFR/ERK/p38 MAPK and PI3K/Akt were increased and that activated caspase-3 and ICAM-1 mRNA were decreased after knockdown of miR155. In conclusion, knockdown of miR155 could modulate ROS production, NO generation, apoptosis and function of HBMECs via regulating diverse gene expression, such as caspase-3, ICAM-1 and EGFR/ERK/p38 MAPK and PI3K/Akt pathways. J. Cell. Biochem. 116: 2870–2881, 2015.

KEY WORDS: miR155; ISCHEMIC STROKE; HUMAN BRAIN MICROVESSEL ENDOTHELIAL CELLS; CELL FUNCTION; REGULATORY MECHANISM; OXIDATIVE STRESS

Vascular endothelial cells (ECs) are important in the regulation of vascular function and homeostasis [Vanhoutte et al., 2009]. Endothelial dysfunction, defined as impairments in endothelium-dependent vasodilatation, angiogenesis, anti-thrombogenesis, and anti-inflammation, is associated with reactive oxygen species (ROS) overproduction [Erusalimsky and Skene, 2009] and nitric oxide (NO) reduction [Hayashi et al., 2006]. It is believed that endothelial dysfunction is the common character and could be the potential preventive and therapeutic target of vascular diseases such as atherosclerosis and ischemic stroke [Arai et al., 2009; Qin et al., 2012; Leung and Jensen, 2013].

Various genes have been indicated to participate in the control of endothelial functions. Membrane phosphatidylinositol-3-kinase (PI3K) and serine/threonine kinase (Akt) are the upstream regulators of eNOS activation which is important for NO production in endothelial cells [Bohlen et al., 2009; Morello et al., 2009]. It has been suggested that ischemic preconditioning protects endothelial function via inhibition of oxidative stress and activation of PI3K/

Y. Liu and Q. Pan contributed equally to this work.

The authors declare that there is no conflict of interests regarding the publication of this paper.

Grant sponsor: National Natural Science Foundation of China; Grant numbers: 81400360, 81270195.

*Correspondence to: Xiaotang Ma, Ph.D. and Yanfang Chen, M.D PhD, Guangdong Key Laboratory of Age-Related Cardiac and Cerebral Diseases, Institute of Neurology, Affiliated Hospital of Guangdong Medical College, Zhanjiang, 524001, China. E-mail: mxtgdmc@163.com and yanfang.chen@wright.edu

Manuscript Received: 9 January 2015; Manuscript Accepted: 14 May 2015

Accepted manuscript online in Wiley Online Library (wileyonlinelibrary.com): 26 May 2015

DOI 10.1002/jcb.25234 • © 2015 Wiley Periodicals, Inc.

Akt/eNOS pathway [Song et al., 2005; He et al., 2013]. Meanwhile, other regulators can also modulate endothelial function. Epidermal growth factor receptor (EGFR)/extracellular regulated protein kinases (ERK), and p38 mitogen-activated protein kinase (p38 MAPK) signaling pathways have been shown to regulate the migration function of endothelial cells [Maretzky et al., 2011; Chen et al., 2014; Kim et al., 2014]. Caspase-3, an important member of the caspase (cysteine aspartic proteinases) family, could play a key role in endothelial cell apoptosis [Lakhani et al., 2006]. Cell adhesion molecules such as vascular cell adhesion molecule (VCAM)-1, intercellular adhesion molecule (ICAM)-1 and E-selectins expressed on endothelial cells have been shown to promote the adhesion of endothelial cells with leukocytes [Hansson et al., 2006], which leads to vascular inflammation [Qin et al., 2012].

MicroRNAs (miRs), single-stranded 20-nucleotide noncoding RNAs, are known to modulate gene expression by their ability to degrade their target messenger RNAs (mRNAs) and/or induce translational repress [Pasquinelli, 2012]. Emerging evidence suggests a possible role of miR155 in vascular diseases. An in vivo study showed that miR155 deficiency enhanced the development and unstability of atherosclerotic plaque in hyperlipidemic mice [Donners et al., 2012]. Several works indicated that miR155 expression was altered in ischemic stroke [Liu et al., 2010; Hunsberger et al., 2012]. Recently, miR155 has been shown to regulate the function and multiple biological pathways of vascular cells. The migration and apoptosis of human umbilical vein endothelial cells (HUVECs) [Ceolotto et al., 2011; Liu et al., 2013b] and vascular adventitial fibroblasts [Zheng et al., 2010] are modulated by miR155 via the type 1 angiotensin II receptor (AT1R) signaling. Meanwhile, miR155 could regulate endothelial inflammation through E26 transformation-specific sequence 1 (ETS-1) [Zhu et al., 2011]. Overexpression of miR155 decreases eNOS expression and NO production in HUVECs [Sun et al., 2012]. However, there is no information regarding the effects and potential mechanisms of miR155 on endothelial cells in the brain.

Oxidized low density lipoprotein (ox-LDL) is well known as one of the risk factors for various vascular diseases [Verhoye et al., 2009]. Elevated levels of circulating ox-LDL increase turbulent blood flow [Inoue et al., 2001] and excessive vascular inflammation [Libby et al., 2009], and impair endothelium-dependent relaxation, contributing to endothelial dysfunction and ischemic stroke [Salvayre et al., 2002; Pirillo et al., 2013]. Evidence has indicated that ox-LDL could compromise the function of ECs by increasing oxidative stress, characterized by the overproduction of ROS, which contributed to cell apoptosis [Cominacini et al., 2000; Napoli, 2003; Hong et al., 2014]. Furthermore, ox-LDL activates ECs by upregulating the expression of several cell surface adhesion molecules which mediates the adhesion of blood leukocytes [Pirillo et al., 2013].

In this study, we investigated the effects of miR155 on the ROS production, NO generation, apoptosis, and function of human brain microvessel endothelial cells (HBMECs) under physiological and ox-LDL-induced pathological conditions. To explore the underlying mechanisms, we analyzed the expression of caspase-3, ICAM-1, VCAM-1, E-selectins, EGFR/ERK/p38 MAPK, and PI3K/Akt pathways.

MATERIALS AND METHODS

CELL CULTURE

HBMECs were obtained from Shanghai Bioleaf Biotech Co. Ltd. The cells were cultured on 100-mm cell culture dishes in DMEM (Hyclone), supplemented with 10% fetal bovine serum (FBS, Hyclone), 100 U/ml penicillin and 100 U/ml streptomycin in a 37°C incubator with humidified atmosphere of 5% CO_2/95% air. HL60 cells were cultured in Medium 1640 (Hyclone) supplemented with 10% fetal bovine serum (FBS, Hyclone), 100 U/ml penicillin and 100 U/ml streptomycin in a 37°C incubator with humidified atmosphere of 5% CO_2/ 95% air.

ESTABLISHMENT OF miR155 SILENCED CELLS

The lentivirus carry green fluorescent protein (GFP) marker for gene expression with miR155 silencing shRNA (Lv-si155) or with scrambled control (Lv-NC) were purchased from GenePharma (Shanghai, China). To obtain miR155 knockdown and control HBMECs, lentivirus Lv-si155 or Lv-NC was used to infect the cells as previously described [Liu et al., 2013a]. Briefly, HBMECs cultured in 6-well plates with 75% confluence were incubated with 1×10^7 infectious units of Lv-si155 or Lv-NC in culture medium for 48 h. After that, the viruses contained medium was replaced with fresh medium. Puromycin (1 μg/ml) was added to select stably transduced HBMECs. The positive cells were observed under a fluorescence microscope, and the efficiency of miR155 knockdown was confirmed by real-time reverse transcription (RT)-polymerase chain reaction (PCR).

REAL-TIME RT-PCR ANALYSIS

Total cell RNAs were extracted using TRIzol reagent (Invitrogen, Carlsbad, CA). The miR155 cDNAs were synthesized from 3 μg total RNA using hairpin-it™ miRNAs RT-PCR Quantitation kit (GenePharma, Shanghai, China) based on manufactory instruments (25°C for 30 min, 42°C for 30 min, and 85°C for 5 min). Real-time PCR parameters were: 95°C for 3 min, 40 cycles were performed at 95°C for 12 s, 60°C for 40 s [Liu et al., 2013a]. PCR primer: 5-GCT TCG GTT AAT GCT AAT CGT G-3 and 5-CAG AGC AGG GTC CGA GGT A-3 for miR155; 5-CTC GCT TCG GCA GCA CA-3 and 5-AAC GCT TCA CGA AYY YGC GT-3 for U6. U6 was chosen as housekeeping gene for normalizing the data of miR155 expression. The cDNAs of ICAM-1, VCAM-1, and E-selections were synthesized from 1 μg total RNA using RevertAid First Strand cDNA Synthesis Kit (Thermo Scientific) at 42°C for 60 min, 70°C for 5 min. Real-time PCR was carried out on a LightCycer480-II System (Roche Diagnostics, Penzberg, Germany) by using SYBR Premix Ex TaqTM (TAKARA, Japan) at 95°C for 30 s, 40 cycles (95°C for 5 s, 60°C for 20 s) as previously described [Palumbo et al., 2000]. Gene specific oligonucleotide were obtained from sangon (QuantiTect Primer Assay). PCR primers: 5-CAA AGG CAG AGT ACG CAA AC-3 and 5-ACA GGA TTT TCG GAG CAG G for VCAM-1; 5-CAA TGT GCT ATT CAA ACT GCC C-3 and 5- CAG CGT AGG GTA AGG TTC TTG-3 for ICAM-1; 5-AAG TTC GCC TGT CCT GAA G-3 and 5-CAG AAA GTC CAG CTA CCA AGG-3 for E-selectins; 5-GAA GGG CTC ATG ACC ACA GTC CAT-3 and 5-TCA TTG TCG TAC CAG GAA ATG AGC TT-3 for GAPDH. GAPDH was used as

housekeeping gene for normalizing the data of ICAM-1, VCAM-1 and E-selectins expression. Each experiment was repeated three times. The relative quantification of the gene expression was determined using the comparative CT method ($2^{-\triangle\triangle Ct}$).

MEASUREMENT OF ROS

Intracellular ROS production was determined by dihydroethidium (DHE) (Beyotime, China) staining followed by flow cytometric analysis [Wang et al., 2013]. Briefly, HBMECs were grown to confluence on 6-well cell culture plate, stimulated with ox-LDL (10 μg) or vehicle for 24 h, then incubated with 5 μM DHE solution at 37°C for 2 h and washed with PBS twice. The fluorescence intensity of cells was analyzed by flow cytometry. For pathway blocking experiments, cells were pre-incubated with PI3K inhibitor (LY294002, 20 μM; Selleckchem) for 2 h.

MEASUREMENT OF NO

As described previously [Wang et al., 2013], total NO production in cells was determined by measuring the concentration of nitrate and nitrite (a stable metabolite of NO) using the Total Nitric Oxide Assay Kit (Beyotime, China). For pathway blocking experiments, cells were pre-incubated with LY294002 (20 μM) for 2 h.

HOECHST 33258 STAINING ANALYSIS OF CELL APOPTOSIS

Cell apoptosis was analyzed by Hoechst 33258 staining as previously described [Zhu et al., 2004]. In brief, the ox-LDL and serum deprivation (SD) medium was used for inducing apoptosis [Lee et al., 2010; Hou et al., 2014]. Cells of each group seeded on sterile cover glasses were placed in 6-well plates for culture in DMEM medium supplemented with 10% FBS (vehicle) or added 10 μg ox-LDL, or SD medium with 10 μg ox-LDL (SD + ox-LDL) or none (SD) for 48 h. After that, cells were fixed, washed with PBS and stained with Hoechst 33258 staining solution according to the manufacturer's instructions (Beyotime) and observed under a fluorescence microscope. Five independent fields were assessed for each well, and the average number of positive cells and total cells per field (magnification, 200×) were determined. The apoptosis rate of cells was defined as the ratio of positive cells versus total cells.

ANNEXIN V-PE/7-AAD STAINING ANALYSIS OF CELL APOPTOSIS

Cells of each group seeded on sterile cover glasses were placed in 6-well plates for culture in DMEM medium supplemented with 10% FBS (vehicle) or added 10 μg ox-LDL, or SD medium with 10 μg ox-LDL (SD + ox-LDL) or none (SD) for 48 h. The apoptosis assay of HBMECs was conducted with using an Annexin V-PE/7-AAD apoptosis detection kit (BD Biosciences). Briefly, cells were washed with PBS, resuspended with 100 μl 1× annexin-binding buffer, incubated with 5 μl PE-conjugated Annexin V and 5 μl 7-Amino-actinomycin (7-AAD) for 15 min in the dark, then analyzed by flow cytometry. Cells stained with both Annexin V-PE and 7-AAD were considered to be late apoptotic HBMECs, and the cells stained only with Annexin V-PE were considered to be early apoptotic HBMECs [Gao et al., 2013]. The experiment was repeated three times. And three plates per experiment were analyzed in each group.

CELL PROLIFERATION ASSAY

Proliferative capability of HBMECs was tested by MTT (3-[4,5-dimethylthiazyol-2yl] -2,5-diphenyltetrazolium bromide) (Sigma, 5 mg/ml) assay [Liu et al., 2013b]. HBMECs were seeded at 2×10^3/well in 96-well plate and cultured in 100 μl DMEM (supplemented with 10% FBS) with ox-LDL (10 μg) or vehicle. MTT solution (20 μl) was added and incubated with cells for 4 h at 37°C, then 150 μl DMSO was added to each well, and incubated with the cells for 20 min at 37°C. The optical density (OD) value of cells was read at 490 nm in a microplate reader (BioTek). Measurement was carried out from day 1 to day 5. Cells in triplicate wells were examined at each time point, and the experiment was repeated three times. Results were calculated from the values obtained in three independent experiments.

CELL MIGRATION ASSAY

The migration distance of HBMECs was measured by scratch assay [Zhu et al., 2011]. HBMECs were grown to confluence on 6-well cell culture plate. A scratch was made through the cell monolayer using a P200 pipette tip. After washing with PBS, cells were cultured in 0.5% FBS maintenance medium with 10 μg ox-LDL or vehicle. Photographs of the wounded area were taken immediately (0 h) and 16 h after making the scratch to monitor the invasion of cells into the scratched area (magnification, 40×).

TUBE FORMATION ASSAY

The tube formation ability was evaluated by using the tube formation assay kit (Chemicon) as we previously described [Wang et al., 2013]. Briefly, EC Matrix working solution was placed in a 96-well tissue culture plate at 37°C for 1 h to allow the matrix solution to solidify. Then the cells were placed (1×10^4 cells/well) onto the surface of the solidified EC Matrix and incubated with endothelial cell growth medium-2 (EGM-2) (Longza) containing ox-LDL (10 μg) or vehicle for 24 h at 37°C. Tube formation was evaluated with an inverted light microscope. A structure exhibiting a length three times its width was defined as a tube. Five independent fields were assessed for each well, and the average number of tubes per field (magnification, 200×) was determined.

CELL ADHESION ASSAY

Cell adhesion ability was evaluated as previously reported [Zhu et al., 2011]. Briefly, HBMECs were grown to confluence on 24-well cell culture plate, stimulated with ox-LDL(10 μg) or vehicle for 24 h. Then, the HL60 cells (1×10^4/well) labeled with acridine orange (Sigma) were added into each well. After 1 h (37°C) incubation of HL60 cells with confluent HBMECs monolayer, the media containing non-attached HL60 cells was removed, and the wells were washed twice with PBS. The number of HL60 cells adhering to HBMECs was counted in five images of random fields captured by a microscope (magnification, 100×). Cell adhesion ability was defined as the average number of HL60 cells/field.

WESTERN BLOT ANALYSIS

For western blot analysis, total cell proteins (40 mg) extracted from each group were separated by 12% SDS–PAGE on tris-glycine gels (Invitrogen) and transferred to polyvinylidene difluoride membranes

(Millipore Corp, Bedford, MA). After blocking at room temperature (RT) in TBS (50 mM Tris, 150 mM NaCl, pH 7.6, 5% fat-free dry milk) for 1 h, the membranes were washed in TBST (0.5% Tween20 in TBS) at RT. Primary antibody was added over night at 4°C. Following extensive washing, membranes were incubated with secondary antibody (1:50,000, EarthO*x*, San Francisco, CA) for 1 hr at RT. After washing three times for 30 min with TBST, the immunoreactivity was visualized by ECL solution (Amersham, Sweden). Beta actin (1:1000, EarthOx, San Francisco, CA) was used to normalize protein loading. The following primary antibodies were used: EGF receptor and phosho-EGF receptor (Tyr1068) (1:1000, Invitrogen, Carlsbad, CA), Erk1/2 and phosphor-Erk1/2 (Thr202/Tyr204) (1:1000, CST), p38 MAPK and pho-p38 MAPK (1:1000, CST), Caspase-3 (1:1000, CST), PI3 kinase p110a (1:1000, CST), Akt and phosphor-Akt (1:1000, CST).

STATISTIC ANALYSIS

Data were expressed as mean ± SD. Comparisons for two groups were performed by using a Student's *t*-test (GraphPad Prism 5 software). Multiple comparisons were performed by two-way ANOVA. *P*-values <0.05 were considered to be significant.

RESULTS

MiR155 WAS SUCCESSFULLY KNOCKED DOWN IN HBMECS BY Lv-si155

Figure 1A showed GFP (maker gene) expression on HBMEC cells, demonstrating the success of lentivirus stable infection. The efficiency of miR155 silencing was evaluated by real-time PCR analysis. The value of miR155 in the HBMECs infected with Lv-NC (HBMEC-NC) was set as the control. The level of miR155 in HBMECs infected with Lv-si155 (HBMEC-si155) was significantly reduced to about 35% of HBMEC-NC (HBMEC-si155 *vs.* HBMEC-NC, $P<0.01$; Fig. 1B).

SILENCING OF miR155 DECREASED ROS PRODUCTION AND INCREASED NO PRODUCTION VIA PI3K/Akt SIGNALING PATHWAY

Flow cytometric analysis demonstrated that ox-LDL (10 μg) induced ROS production in both HBMEC-NC and HBMEC-si155 cells (vs. vehicle; $P<0.01$; Fig. 2A). Knockdown of miR155 reduced ROS production in both vehicle and ox-LDL treated cells (vs. HBMEC-NC; $P<0.01$; Fig. 2A). In contract, ox-LDL decreased the NO production in both HBMEC-NC and HBMEC-si155 cells (vs. vehicle; $P<0.01$; Fig. 2B), whereas silencing of miR155 increased NO production in both vehicle and ox-LDL treated cells (vs. HBMEC-NC; $P<0.01$; Fig. 2B). In addition, PI3K inhibitor LY294002 (20 μM) abrogated the inhibitory effect of miR155 knockdown on ROS production in both vehicle and ox-LDL treated cell (vs. HBMEC- si155; $P<0.01$; Fig. 2A), whereas it inhibited miR155 knockdown enhanced NO production in both vehicle and ox-LDL treated cell (vs. HBMEC- si155; $P<0.01$; Fig. 2B). These data suggested that PI3K signaling was involved in the effects of miR155 on NO production and ROS generation in HBMECs at basal and ox-LDL challenged condition.

To investigate the signal pathways associated with miR155, we examined the expression of PI3K, Akt, and the activity of Akt (p-Akt/Akt) in HBMECs. Western blot analysis revealed that the levels of PI3K and p-Akt/Akt in both HBMEC-NC and HBMEC-si155 cells (vs. vehicle; $P<0.01$; Fig. 2C) were decreased by ox-LDL. However, silencing of miR155 increased the levels of PI3K and p-Akt/Akt in both ox-LDL and vehicle treated HBMECs (vs. HBMEC-NC; $P<0.01$; Fig. 2C) . Furthermore, the effects of miR155 on p-Akt and Akt expression were inhibited by PI3K inhibition (LY294002, 20 μM) (vs. HBMEC- si155; $P<0.01$; Fig. 2C).

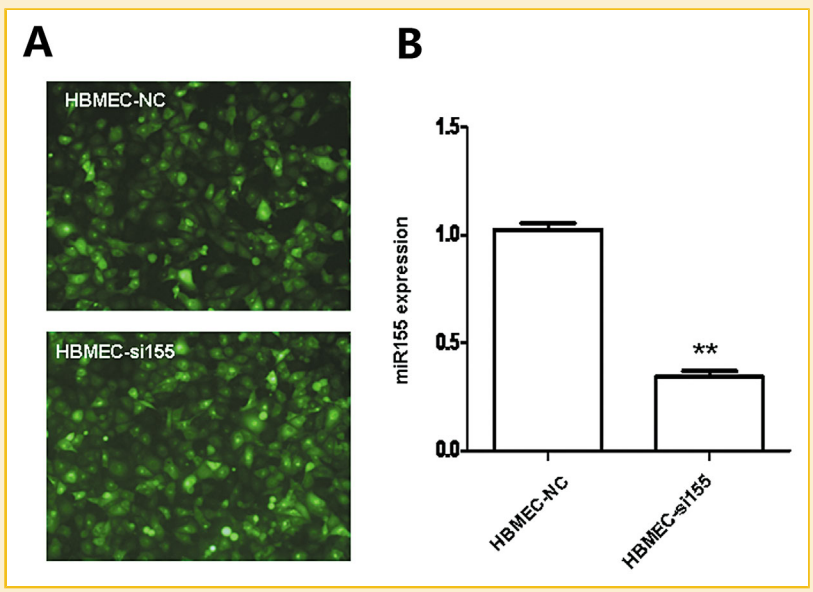

Fig. 1. Knockdown of miR155 in HBMECs by lentivirus mediated shRNA transfection. (A) Microscopic images of GFP marker expression in HBMECs after lentivirus transfection. (B) Real-time PCR analysis of miR155 expression in HBMECs infected with Lv-si155 and Lv-NC. $^{**}P<0.01$, versus HBMEC-NC; n = 3/groups.

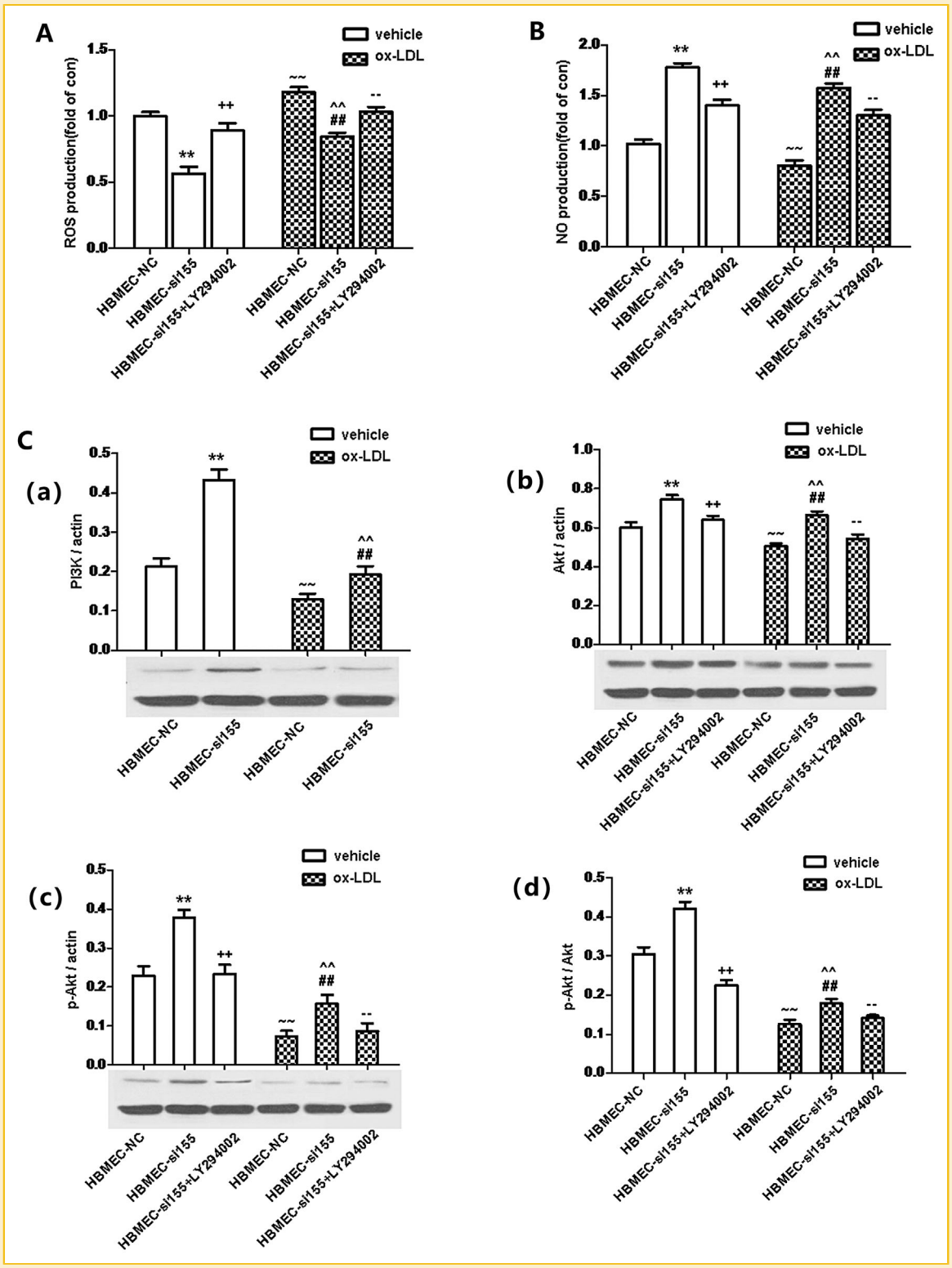

Fig. 2. Effects of ox-LDL(10 μg) and miR155 deficiency on ROS and NO production, PI3K and p-Akt/Akt expression in HBMECs. (A) ROS production. (B) NO generation of HBMECs. (C) Expression of PI3K and p-Akt/Akt. $^{\sim\sim}P < 0.01$, versus HBMEC-NC, vehicle; $^{\wedge\wedge}P < 0.01$, versus HBMEC-si155, vehicle; $^{**}P < 0.01$, versus HBMEC-NC, vehicle; $^{\#\#}P < 0.01$, versus HBMEC-NC, ox-LDL; $^{++}P < 0.01$, versus HBMEC- si155, vehicle; $^{--}P < 0.01$, versus HBMEC- si155, ox-LDL; n = 3/group.

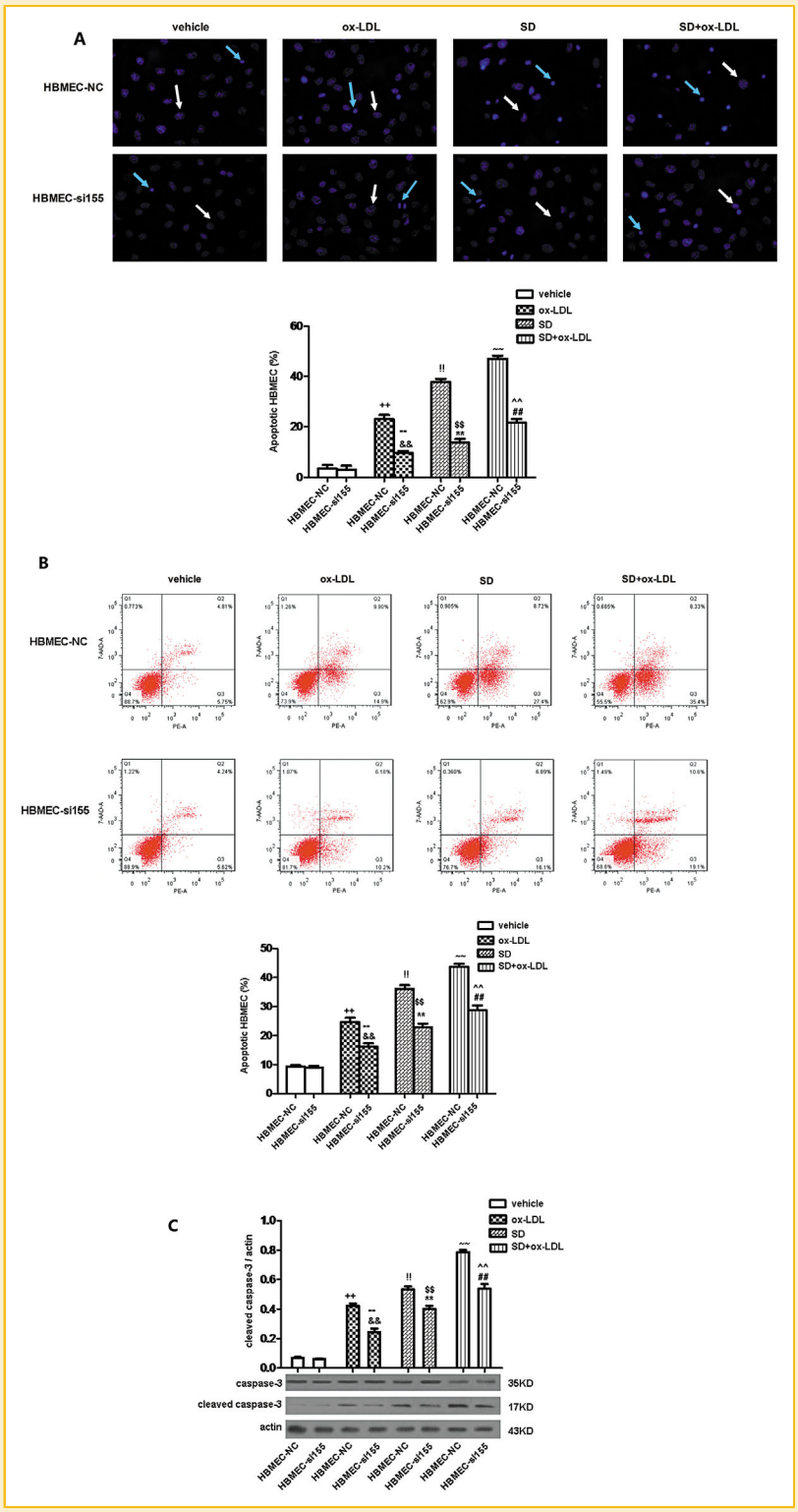

Fig. 3. Effects of ox-LDL(10 μg)/serum deprivation (SD)/SD plus ox-LDL and miR155 deficiency on HBMEC apoptosis and cleaved caspase-3 expression. (A) HBMEC apoptosis monitored by Hoechst 33258 staining (blue arrows represent apoptotic cells, white arrows represent normal cells). (B) HBMEC apoptosis determined by flow cytometric analysis. (C) Expression of cleaved caspase-3 protein in HBMECs. $^{++}P < 0.01$, versus HBMEC-NC, vehicle; $^{-}P < 0.01$, versus HBMEC- si155, vehicle; $^{\&\&}P < 0.01$, versus HBMEC-NC, vehicle; $^{!!}P < 0.01$, versus HBMEC-NC, vehicle; $P < 0.01$, versus HBMEC- si155, vehicle; $^{\sim\sim}P < 0.01$, versus HBMEC-NC, SD; $^{\wedge\wedge}P < 0.01$, versus HBMEC-si155, SD; $^{**}P < 0.01$, versus HBMEC-NC, SD; $^{\#\#}P < 0.01$, versus HBMEC-NC, SD + ox-LDL; n = 3/group.

SILENCING OF miR155 REDUCED THE APOPTOSIS OF HBMECs

Hoechst 33258 staining and Annexin V-PE/7-AAD analysis revealed that both ox-LDL (10 μg) and SD promoted HBMEC apoptosis (vs. vehicle; $P < 0.01$; Fig. 3A and B) and ox-LDL increased the SD induced apoptotic rate in both HBMEC-NC and HBMEC-si155 cells (vs. SD; $P < 0.01$; Fig. 3A and B). In addition, we monitored the cleaved caspase-3 levels, which are associated with induction of apoptosis, by western blot. Result showed that cleaved caspase-3 protein expression was significantly increased after ox-LDL or SD treatment (vs. vehicle; $P < 0.01$; Fig. 3C), and ox-LDL increased the SD induced caspase-3 activation in both HBMEC-NC and HBMEC-si155 cells (vs. SD; $P < 0.01$; Fig. 3C). However, knockdown of miR155 decreased cell apoptosis (vs. HBMEC-NC; $P < 0.01$; Fig. 3A and B) and cleaved caspase-3 protein expression (vs. HBMEC-NC; $P < 0.01$; Fig. 3C) in ox-LDL, SD and SD plus ox-LDL treated HBMECs. These results suggest that miR155 might promote apoptosis of HBMECs and caspase-3 activation.

SILENCING OF miR155 INCREASED THE PROLIFERATION OF HBMECs

MTT cell proliferation assay showed that ox-LDL (10 μg) markedly increased the proliferation of both HBMEC-NC and HBMEC-si155 cells in days 3–5 (vs. vehicle; $P < 0.01$; Fig. 4). Knockdown of miR155 further increased HBMECs cell proliferation of days 3–5 whether with ox-LDL treatment or not (vs. HBMEC-NC; $P < 0.01$; Fig. 4).

DOWNREGULATION OF MIR155 INCREASED THE MIGRATION OF HBMECS AND THE EXPRESSION OF EGFR/p-EGFR, ERK1/2/p-ERK1/2, p38/P-p38 MAPK

Scratch assays analysis identified that the migration of HBMECs-si155 was increased compared with HBMEC-NC (vs. HBMEC-NC; $P < 0.01$; Fig. 5A). Ox-LDL (10 μg) promoted the migration of HBMEC-NC and HBMEC-si155 (vs. vehicle; $P < 0.01$; Fig. 5A), and miR155 knockdown could significantly improve the ability of cell migration (vs. HBMEC-NC; $P < 0.01$; Fig. 5A).

Since phosphorylation of EGFR and its downstream MAP kinases ERK1/2 and p38MAPK are critical in regulating cell migration [Zhu et al., 2011; Claude et al., 2014], we investigated the signal pathways associated with the ability of miR155 in regulating HBMECs migration by using western blotting analyses. We found that ox-LDL (10 μg) could increased the levels of EGFR, ERK1/2, p38 MAPK and their phosphorylation in both HBMEC-NC and HBMEC-si155 cells (vs. vehicle; $P < 0.01$; Fig. 5B). Knockdown of miR155 increased the levels of those proteins in HBMEC cells in both vehicle and ox-LDL treated cells (vs. HBMEC-NC; $P < 0.01$; Fig. 5B). Although activity of ERK (p-ERK/ERK) was decreased in HBMEC-si155 in the vehicle group, the activity of p38 and EGFR were upregulated by silencing of miR155 (vs. HBMEC-NC; $P < 0.01$; Fig. 5B).

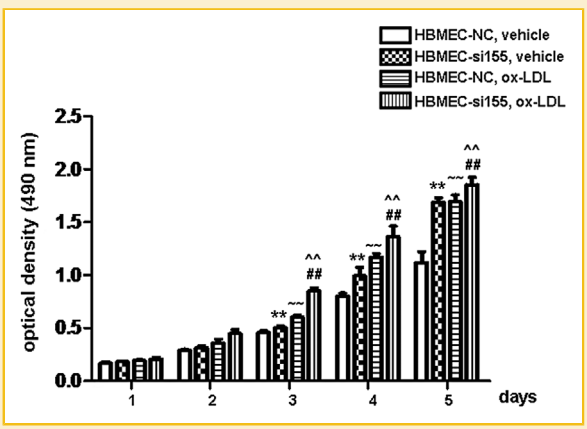

Fig. 4. Ox-LDL(10 μg) and miR155 silencing promoted HBMECs proliferation. $^{\sim\sim}P < 0.01$, versus HBMEC-NC, vehicle; $^{\wedge\wedge}P < 0.01$, versus HBMEC-si155, vehicle; $^{**}P < 0.01$, versus HBMEC-NC, vehicle; $^{\#\#}P < 0.01$, versus HBMEC-NC, ox-LDL; n = 3/group.

DOWNREGULATION OF miR155 INCREASED TUBE FORMATION ABILITY OF HBMECs

As shown in Figure 6, knockdown of miR155 increased the tube formation ability of HBMECs (vs. HBMEC-NC; $P < 0.01$; Fig. 6). Ox-LDL (10 μg) decreased the tube formation ability of HBMECs (vs. vehicle; $P < 0.01$; n = 3/group; Fig. 6). However, miR155 silencing could improve the tube formation ability of HBMECs impaired by ox-LDL (vs. HBMEC-NC; $P < 0.01$; Fig. 6).

SILENCING miR155 DECREASED THE ADHESION OF HBMECS WITH HL60 CELLS AND THE EXPRESSION OF ICAM-1 mRNA

Cell adhesion assay was used to explore the influence of miR155 on the interaction of endothelial cells with leukocytes. As we expected, ox-LDL (10 μg) increased the adhesion of HBMECs with HL60 cells in both HBMEC-NC and HBMEC-si155 cells (vs. vehicle; $P < 0.01$; Fig. 7A). Silencing miR155 markedly decreased the number of HL60 cells adhered to HBMECs (vs. HBMEC-NC; $P < 0.01$; Fig. 7A).

We further determined ICAM-1, VCAM-1, E-selectins mRNA expression by quantitative PCR. Our experimental results showed that ox-LDL (10 μg) increased ICAM-1 mRNA expression in both HBMEC-NC and HBMEC-si155 cells (vs. vehicle; $P < 0.01$; Fig. 7B). Meanwhile, ICAM-1 mRNA was decreased markedly after knocking down of miR155 in HBMECs or HBMECs treated with ox-LDL (vs. HBMEC-NC; $P < 0.01$; Fig. 7B). There was no significant difference in VCAM-1 or E-selectins mRNA expression between HBMEC-si155 and HBMEC-NC (vs. HBMEC-NC; $P > 0.05$; Fig. 7B).

DISCUSSION

In this study, we investigated the effects of miR155 on various activities of HBMECs under normal and ox-LDL induced oxidative stress situations. Firstly, we found that deficiency of miR155 could reduce ROS production and promote NO generation in HBMECs. More importantly, miR155 deficiency could resist ox-LDL induced ROS overproduction and NO reduction in HBMECs. Moreover, we demonstrated that the effects of miR155 knockdown on ROS production and NO generation were via the PI3K/Akt signaling pathway. Secondly, functional studies revealed that knockdown of miR155 deceased cell apoptosis, increased cell proliferation, and enhanced the abilities in migration and tube formation under normal and ox-LDL treatment conditions. These changes were associated with down-regulating of caspase-3 expression and up-regulation of EGFR, ERK1/2 and p38 MAPK expression and phosphorylation.

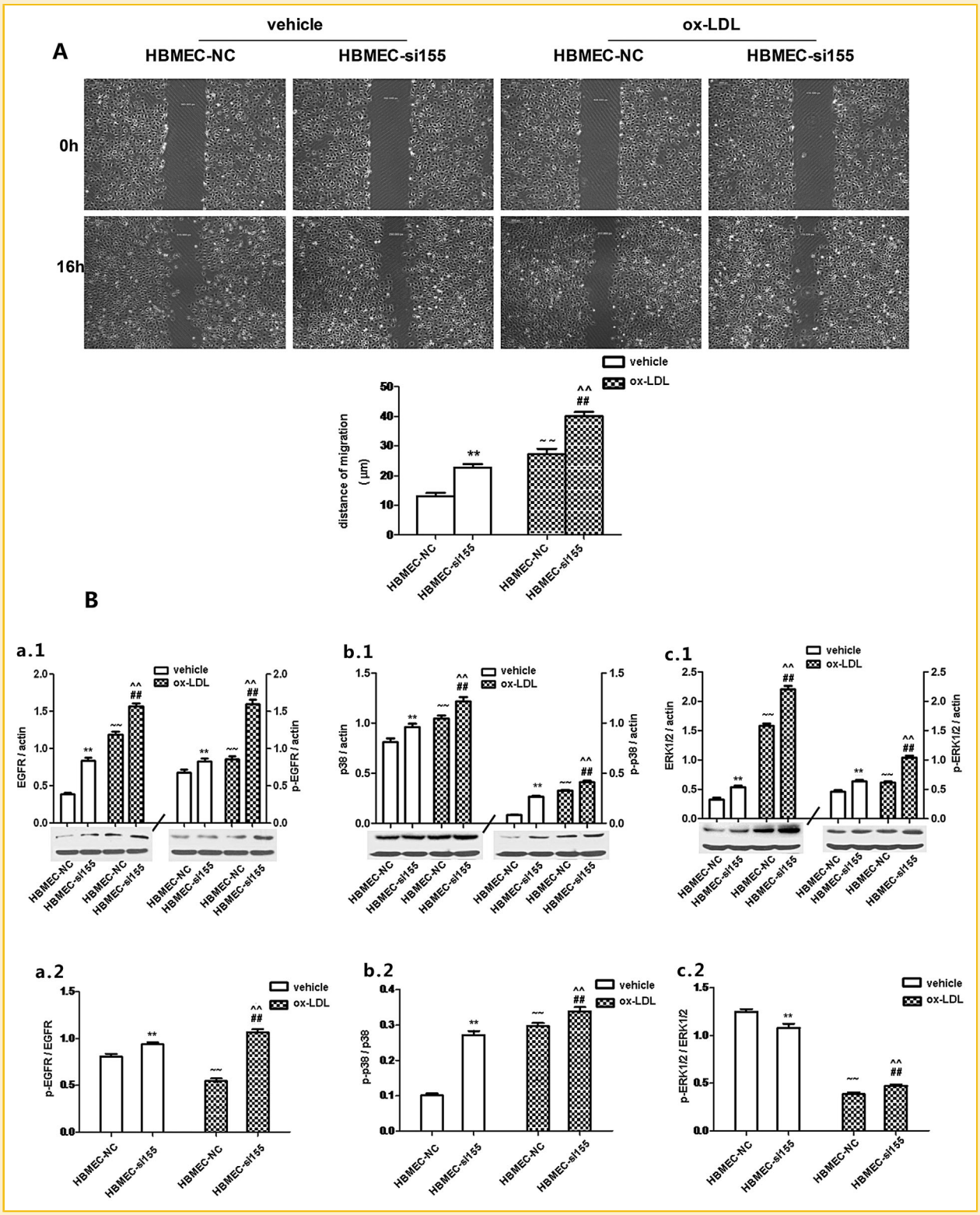

Fig. 5. Ox-LDL(10 μg) and miR155 deficiency increased the migration of HBMECs and expression of p-EGFR/EGFR, p-p38/p38, p-ERK1/2/ERK1/2. (A) Migration of HBMECs in a monolayer scrape injury assay. (B) Expression of p-EGFR/EGFR, p-p38/p38, p-ERK1/2/ERK1/2. $^{\sim\sim}P < 0.01$, versus HBMEC-NC, vehicle; $^{\wedge\wedge}P < 0.01$, versus HBMEC-si155, vehicle; $^{**}P < 0.01$, versus HBMEC-NC, vehicle; $^{\#\#}P < 0.01$, versus HBMEC-NC, ox-LDL; n = 3/group.

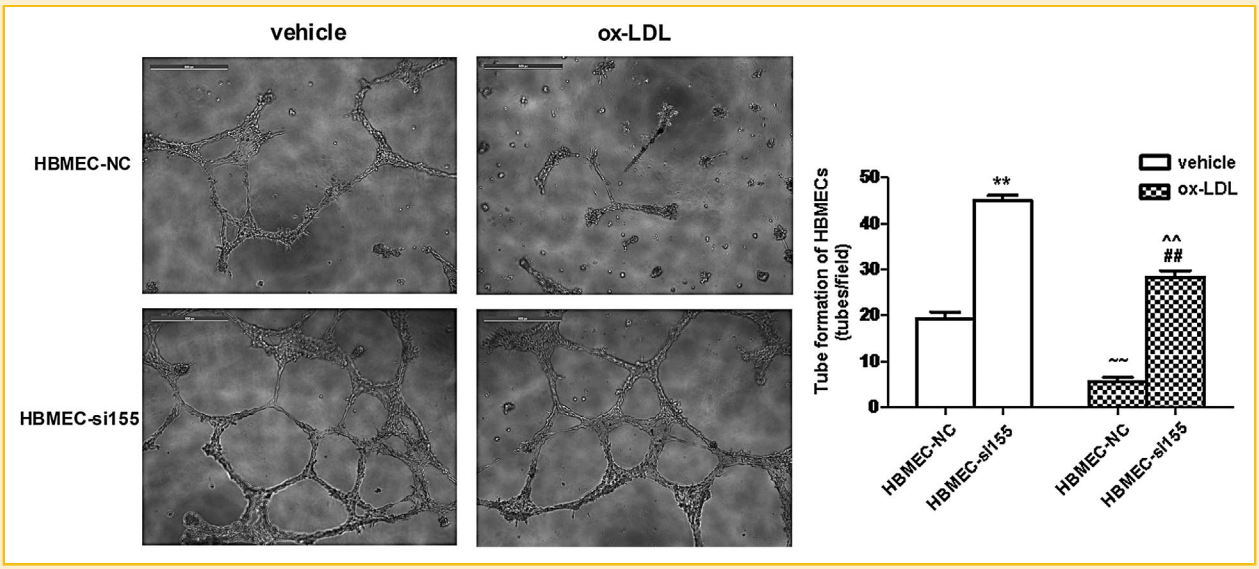

Fig. 6. Effects of ox-LDL(10 μg) and miR155 deficiency on tube formation abilities of HBMECs. $^{\sim\sim}P<$n0.01, versus HBMEC-NC, vehicle; $^{\wedge\wedge}P<0.01$, versus HBMEC-si155, vehicle; $^{**}P<$n0.01, versus HBMEC-NC, vehicle; $^{\#\#}P<0.01$, versus HBMEC-NC, ox-LDL; n = 3/group.

Finally, in normal or oxidative stress situations, miR155 silencing could inhibit the adhesion of HBMECs with HL60 cells and decrease ICAM-1 expression in HBMECs.

Oxidative stress is an important mechanism of vascular disease, and it occurs when there is an imbalance between the generation of reactive oxygen and the antioxidant defense systems in the body [Magenta et al., 2013]. As an important signaling molecule for oxidative stress, ROS is known to impair cell function, contributing to diseases [Cai and Harrison, 2000]. Excessive ROS can oxidize various molecules, which could induce overexpression of redox genes, intracellular calcium overload, and DNA fragmentation, resulting in damage to ECs [Higashi et al., 2009]. NO can reduce the production of ROS [Chavakis et al., 2001; Hayashi et al., 2006]. When oxidative stress and the aberrant production of ROS occurs, NO is decreased [Chavakis et al., 2001; Hayashi et al., 2006]. Although it remains unclear how NO can reduce ROS production, NO-mediated ROS reduction may be at least due to its direct ROS scavenging action and NADPH oxidase inhibition. Selemidis et al. have reported that NO suppresses NADPH oxidase-dependent superoxide production through S-nitrosylation of p47phox in human endothelial cells [Selemidis et al., 2007]. Thus, the ROS overproduction and NO reduction could contribute to the mechanism of endothelial dysfunction. In this study, we found that knockdown of miR155 could reduce ROS production and promote NO generation, indicating the protective effect of miR155 deficiency. In addition, evidence has indicated that ox-LDL, a risk factor of endothelial dysfunction, increases oxidative stress in endothelial cells [Colles et al., 2001; Salvayre et al., 2002; Napoli, 2003; Hong et al., 2014]. In consistent with previous studies, we found that ox-LDL increased ROS and decreased NO production in HBMECs. More interestingly, our data firstly showed that deficiency of miR155 could resist ox-LDL induced ROS production and NO reduction. Research indicates that ROS can alter vascular reactivity, breakdown of the blood-brain barrier and focal destructive lesions, participated in the pathogenesis of ischemic stroke [Allen and Bayraktutan, 2009]. Whereas NO can regulate vascular tone and blood pressure, a risk factor of ischemic stroke. Therefore, miR155 might promote the occurring and developing of ischemic stroke via increasing the production of ROS and reducing NO generation.

As other miRs, miR155 could modulate gene expression by the ability to degrade its target mRNAs and/or induce translational repress. In this study, we found that knockdown of miR155 increased the expression of PI3K and p-Akt/Akt in HBMECs and that PI3K inhibition could decrease the effects of miR155 knockdown on ROS and NO production of HBMECs. These results demonstrated that miR155 modulates ROS production and NO generation via inhibiting the PI3K/Akt signaling cascades in HBMECs. These changes could result in breakdown of the blood-brain barrier and focal vascular dysfunction, and might participate in the pathogenesis of ischemic stroke [Allen and Bayraktutan, 2009].

Our data showed that knockdown of miR155 could decrease ox-LDL/SD/SD + ox-LDL-induced apoptosis in HBMECs. This might relate with the effects of miR155 deficiency on inhibiting ROS and promoting NO production which have been found in our study. As an important signaling molecule for oxidative stress, ROS plays a causal role in endothelial dysfunction and apoptosis [Hayashi et al., 2006]. Whereas NO plays an important role in maintaining vascular homeostasis, and resisting cells apoptosis via reducing ROS production [Chavakis et al., 2001; Hayashi et al., 2006]. The data suggest the anti-apoptotic effect of miR155 deficiency on HBMECs. The effect of miR155 on HBMECs apoptosis is further supported by our observation that miR155 silencing significantly decreased the protein expression of cleaved caspase-3, an apoptosis-promoting factor.

The effects of miR155 on HBMEC cell function were also investigated. We found that miR155 deficiency could increase

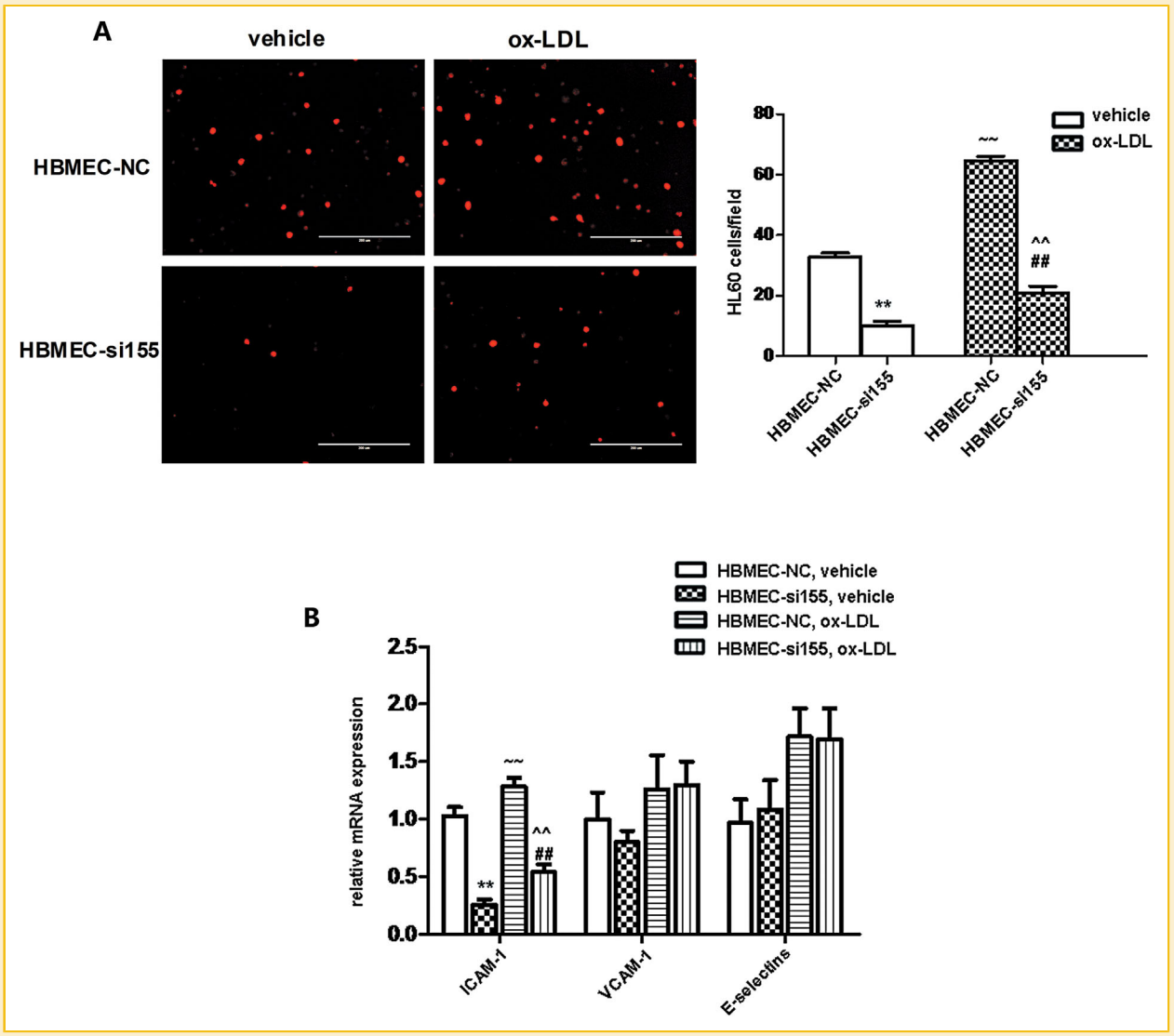

Fig. 7. Effects of ox-LDL(10 μg) and miR155 deficiency on HL60 cells adhered to HBMECs and expression of ICAM-1, VCAM-1, E-selectins. (A) HL60 cells adhered to HBMECs. (B) Expression of ICAM-1, VCAM-1, E-selectins. $^{\sim\sim}P < 0.01$, versus HBMEC-NC, vehicle; $^{\wedge\wedge}P < 0.01$, versus HBMEC-si155, vehicle; $^{**}P < 0.01$, versus HBMEC-NC, vehicle; $^{\#\#}P < 0.01$, versus HBMEC-NC, ox-LDL; n = 3/group.

proliferation while enhance migration and tube formation of HBMECs under normal and ox-LDL treatment conditions. What to be note is that ox-LDL was found to increase the proliferation and migration of HBMECs, which seems contrary to the finding that ox-LDL decreased the tube formation of HBMECs. In fact, previous studies have reported the effects of ox-LDL on promoting proliferation and/or migration of human coronary artery smooth muscle cells and endothelial cells [Inoue et al., 2001; Liu et al., 2014]. However, ox-LDL-induced HBMEC apoptosis might exceed the effect of proliferation, which leads to the decrease in tube formation. Since the proliferation, migration, and tube formation abilities of endothelial cells are associated with angiogenesis, our findings indicate that miR155 could play an important role in repair following ischemic stroke [Arai et al., 2009; Yin et al., 2014]. It should be noted that newly formed blood vessels might lead to plaque formation and plaque rupture [Virmani et al., 2005; Leroyer et al., 2008]. Therefore, miR155 might participate in the occurring and developing of ischemic stroke.

This study also identified some downstream targets of miR155 in regulating HBMEC functions [Maretzky et al., 2011; Chen et al., 2014; Kim et al., 2014]. We found that the expressions of EGFR, ERK1/2, and p38 MAPK, so as the phosphorylation of them were increased after miR155 knockdown. MiR155 deficiency could also increase the activity of EGFR, p38MAPK. However, we found that the activity of ERK (p-ERK/ERK) in HBMECs was decreased when miR155 was silenced. This might be due to the elevation of both ERK and p-ERK with more in ERK. Thus, we consider that the elevation in ERK phosphorylation is differently modulated by miR155 silencing. The results on these signaling pathways help to understand the findings in functional study.

Moreover, it has been reported that activated endothelial cells express adherent molecules which promotes leukocytes adhesion [Qin et al., 2012]. In this study, we found that silencing of miR155 decreased the number of HL60 cells adhered to HBMECs, which was associated with the downregulation of an important adherent molecule, ICAM-1. These indicated that miR155 could increase EC inflammation which contributes significantly to ischemic stroke [Fann et al., 2013; Nakase et al., 2008]. In addition, deficiency of miR155 has been shown to reduce the expression of Bcl6, a nuclear factor-κB antagonist in macrophages [Nazari-Jahantigh et al., 2012], indicating a pro-inflammatory effect of miR155.

CONCLUSION

Our data demonstrate that miR155 plays an important role in controlling ROS and NO production in HBMECs and their diverse functions including cell proliferation, survival, migration, and adhesion under physiological and pathological conditions such as ischemia and ox-LDL stimulation. The underlying mechanisms could include the modulation of caspase-3, ICAM-1, and PI3K/Akt and EGFR/ERK/p38 MAPK pathways. These findings indicate that miR155 have various detrimental effects on brain endothelial cells. Taken our in vitro data together with previous studies by others as we discussed above, miR155 might participate in the pathogenesis of ischemic stroke by impairing ECs functions, vessel repair, and promoting endothelial inflammation and it might be a potential therapeutic targets for ischemic stroke which await further explorations in animal studies and clinical sets.

ACKNOWLEDGMENT

This work was supported by National Natural Science Foundation of China (NSFC, #81400360, #81270195).

REFERENCES

Allen CL, Bayraktutan U. 2009. Oxidative stress and its role in the pathogenesis of ischaemic stroke. Int J Stroke 4:461–470.

Arai K, Jin G, Navaratna D, Lo EH. 2009. Brain angiogenesis in developmental and pathological processes: Neurovascular injury and angiogenic recovery after stroke. FEBS J 276:4644–4652.

Bohlen HG, Zhou X, Unthank JL, Miller SJ, Bills R. 2009. Transfer of nitric oxide by blood from upstream to downstream resistance vessels causes microvascular dilation. Am J Physiol Heart Circ Physiol 297:H1337–H1346.

Cai H, Harrison DG. 2000. Endothelial dysfunction in cardiovascular diseases: the role of oxidant stress. Circ Res 87:840–844.

Ceolotto G, Papparella I, Bortoluzzi A, Strapazzon G, Ragazzo F, Bratti P, Fabricio AS, Squarcina E, Gion M, Palatini P, Semplicini A. 2011. Interplay between miR-155, AT1R A1166C polymorphism, and AT1R expression in young untreated hypertensives. Am J Hypertens 24:241–246.

Chavakis E, Dernbach E, Hermann C, Mondorf UF, Zeiher AM, Dimmeler S. 2001. Oxidized LDL inhibits vascular endothelial growth factor-induced endothelial cell migration by an inhibitory effect on the Akt/endothelial nitric oxide synthase pathway. Circulation 103:2102–2107.

Chen Z, Cai Y, Zhang W, Liu X, Liu S. 2014. Astragaloside IV inhibits platelet-derived growth factor-BB-stimulated proliferation and migration of vascular smooth muscle cells via the inhibition of p38 MAPK signaling. Exp Ther Med 8:1253–1258.

Claude S, Boby C, Rodriguez-Mateos A, Spencer JP, Gerard N, Morand C, Milenkovic D. 2014. Flavanol metabolites reduce monocyte adhesion to endothelial cells through modulation of expression of genes via p38-MAPK and p65-Nf-kB pathways. Mol Nutr Food Res 58:1016–1027.

Colles SM, Maxson JM, Carlson SG, Chisolm GM. 2001. Oxidized LDL-induced injury and apoptosis in atherosclerosis. Potential roles for oxysterols. Trends Cardiovasc Med 11:131–138.

Cominacini L, Pasini AF, Garbin U, Davoli A, Tosetti ML, Campagnola M, Rigoni A, Pastorino AM, Lo Cascio V, Sawamura T. 2000. Oxidized low density lipoprotein (ox-LDL) binding to ox-LDL receptor-1 in endothelial cells induces the activation of NF-kappaB through an increased production of intracellular reactive oxygen species. J Biol Chem 275:12633–12638.

Donners MM, Wolfs IM, Stoger LJ, van der Vorst EP, Pottgens CC, Heymans S, Schroen B, Gijbels MJ, de Winther MP. 2012. Hematopoietic miR155 deficiency enhances atherosclerosis and decreases plaque stability in hyperlipidemic mice. PLoS ONE 7:e35877.

Erusalimsky JD, Skene C. 2009. Mechanisms of endothelial senescence. Exp Physiol 94:299–304.

Fann DY, Lee SY, Manzanero S, Chunduri P, Sobey CG, Arumugam TV. 2013. Pathogenesis of acute stroke and the role of inflammasomes. Ageing Res Rev 12:941–966.

Gao J, Zhang C, Fu X, Yi Q, Tian F, Ning Q, Luo X. 2013. Effects of targeted suppression of glutaryl-CoA dehydrogenase by lentivirus-mediated shRNA and excessive intake of lysine on apoptosis in rat striatal neurons. PLoS ONE 8:e63084.

Hansson GK, Robertson AK, Soderberg-Naucler C. 2006. Inflammation and atherosclerosis. Annu Rev Pathol 1:297–329.

Hayashi T, Matsui-Hirai H, Miyazaki-Akita A, Fukatsu A, Funami J, Ding QF, Kamalanathan S, Hattori Y, Ignarro LJ, Iguchi A. 2006. Endothelial cellular senescence is inhibited by nitric oxide: Implications in atherosclerosis associated with menopause and diabetes. Proc Natl Acad Sci USA 103:17018–17023.

He X, Zhao M, Bi XY, Yu XJ, Zang WJ. 2013. Delayed preconditioning prevents ischemia/reperfusion-induced endothelial injury in rats: Role of ROS and eNOS. Lab Invest 93:168–180.

Higashi Y, Noma K, Yoshizumi M, Kihara Y. 2009. Endothelial function and oxidative stress in cardiovascular diseases. Circ J 73:411–418.

Hong D, Bai YP, Gao HC, Wang X, Li LF, Zhang GG, Hu CP. 2014. Ox-LDL induces endothelial cell apoptosis via the LOX-1-dependent endoplasmic reticulum stress pathway. Atherosclerosis 235:310–317.

Hou M, Cui J, Liu J, Liu F, Jiang R, Liu K, Wang Y, Yin L, Liu W, Yu B. 2014. Angiopoietin-like 4 confers resistance to hypoxia/serum deprivation-induced apoptosis through PI3K/Akt and ERK1/2 signaling pathways in mesenchymal stem cells. PLoS ONE 9:e85808.

Hunsberger JG, Fessler EB, Wang Z, Elkahloun AG, Chuang DM. 2012. Post-insult valproic acid-regulated microRNAs: Potential targets for cerebral ischemia. Am J Transl Res 4:316–332.

Inoue M, Itoh H, Tanaka T, Chun TH, Doi K, Fukunaga Y, Sawada N, Yamshita J, Masatsugu K, Saito T, Sakaguchi S, Sone M, Yamahara K, Yurugi T, Nakao K. 2001. Oxidized LDL regulates vascular endothelial growth factor expression in human macrophages and endothelial cells through activation of peroxisome proliferator-activated receptor-gamma. Arterioscler Thromb Vasc Biol 21:560–566.

Kim BS, Park JY, Kang HJ, Kim HJ, Lee J. 2014. Fucoidan/FGF-2 induces angiogenesis through JNK- and p38-mediated activation of AKT/MMP-2 signalling. Biochem Biophys Res Commun 450:1333–1338.

Lakhani SA, Masud A, Kuida K, Porter GA, Jr., Booth CJ, Mehal WZ, Inayat I, Flavell RA. 2006. Caspases 3 and 7: Key mediators of mitochondrial events of apoptosis. Science 311:847–851.

Lee SB, Kim JJ, Kim TW, Kim BS, Lee MS, Yoo YD. 2010. Serum deprivation-induced reactive oxygen species production is mediated by Romo1. Apoptosis 15:204–218.

Leroyer AS, Rautou PE, Silvestre JS, Castier Y, Leseche G, Devue C, Duriez M, Brandes RP, Lutgens E, Tedgui A, Boulanger CM. 2008. CD40 ligand+ microparticles from human atherosclerotic plaques stimulate endothelial proliferation and angiogenesis a potential mechanism for intraplaque neovascularization. J Am Coll Cardiol 52:1302–1311.

Leung WY, Jensen MB. 2013. Histological quantification of angiogenesis after focal cerebral infarction: A systematic review. ISRN Neurol 2013:853737.

Libby P, Ridker PM, Hansson GK. 2009. Inflammation in atherosclerosis: From pathophysiology to practice. J Am Coll Cardiol 54:2129–2138.

Liu DZ, Tian Y, Ander BP, Xu H, Stamova BS, Zhan X, Turner RJ, Jickling G, Sharp FR. 2010. Brain and blood microRNA expression profiling of ischemic stroke, intracerebral hemorrhage, and kainate seizures. J Cereb Blood Flow Metab 30:92–101.

Liu J, Ren Y, Kang L, Zhang L. 2014. Oxidized low-density lipoprotein increases the proliferation and migration of human coronary artery smooth muscle cells through the upregulation of osteopontin. Int J Mol Med 33:1341–1347.

Liu L, Hu Y, Fu J, Yang X, Zhang Z. 2013. MicroRNA155 in the growth and invasion of salivary adenoid cystic carcinoma. J Oral Pathol Med 42:140–147.

Liu T, Shen D, Xing S, Chen J, Yu Z, Wang J, Wu B, Chi H, Zhao H, Liang Z, Chen C. 2013. Attenuation of exogenous angiotensin II stress-induced damage and apoptosis in human vascular endothelial cells via microRNA-155 expression. Int J Mol Med 31:188–196.

Magenta A, Greco S, Gaetano C, Martelli F. 2013. Oxidative stress and microRNAs in vascular diseases. Int J Mol Sci 14:17319–17346.

Maretzky T, Evers A, Zhou W, Swendeman SL, Wong PM, Rafii S, Reiss K, Blobel CP. 2011. Migration of growth factor-stimulated epithelial and endothelial cells depends on EGFR transactivation by ADAM17. Nat Commun 2:229.

Morello F, Perino A, Hirsch E. 2009. Phosphoinositide 3-kinase signalling in the vascular system. Cardiovasc Res 82:261–271.

Nakase T, Yamazaki T, Ogura N, Suzuki A, Nagata K. 2008. The impact of inflammation on the pathogenesis and prognosis of ischemic stroke. J Neurol Sci 271:104–109.

Napoli C 2003. Oxidation of LDL, atherogenesis, and apoptosis. Ann N Y Acad Sci 1010:698–709.

Nazari-Jahantigh M, Wei Y, Noels H, Akhtar S, Zhou Z, Koenen RR, Heyll K, Gremse F, Kiessling F, Grommes J, Weber C, Schober A. 2012. MicroRNA-155 promotes atherosclerosis by repressing Bcl6 in macrophages. J Clin Invest 122:4190–4202.

Palumbo B, Oguogho A, Fitscha P, Sinzinger H. 2000. Prostaglandin E1-therapy reduces circulating adhesion molecules (ICAM-1, E-selectin, VCAM-1) in peripheral vascular disease. Vasa 29:179–185.

Pasquinelli AE 2012. MicroRNAs and their targets: Recognition, regulation and an emerging reciprocal relationship. Nat Rev Genet 13:271–282.

Pirillo A, Norata GD, Catapano AL. 2013. LOX-1, OxLDL, and atherosclerosis. Mediators Inflamm 2013:152786.

Qin B, Yang H, Xiao B. 2012. Role of microRNAs in endothelial inflammation and senescence. Mol Biol Rep 39:4509–4518.

Salvayre R, Auge N, Benoist H, Negre-Salvayre A. 2002. Oxidized low-density lipoprotein-induced apoptosis. Biochim Biophys Acta 1585: 213–221.

Selemidis S, Dusting GJ, Peshavariya H, Kemp-Harper BK, Drummond GR. 2007. Nitric oxide suppresses NADPH oxidase-dependent superoxide production by S-nitrosylation in human endothelial cells. Cardiovasc Res 75:349–358.

Song G, Ouyang G, Bao S. 2005. The activation of Akt/PKB signaling pathway and cell survival. J Cell Mol Med 9:59–71.

Sun HX, Zeng DY, Li RT, Pang RP, Yang H, Hu YL, Zhang Q, Jiang Y, Huang LY, Tang YB, Yan GJ, Zhou JG. 2012. Essential role of microRNA-155 in regulating endothelium-dependent vasorelaxation by targeting endothelial nitric oxide synthase. Hypertension 60:1407–1414.

Vanhoutte PM, Shimokawa H, Tang EH, Feletou M. 2009. Endothelial dysfunction and vascular disease. Acta Physiol (Oxf) 196:193–222.

Verhoye E, Langlois MR, Asklepios I. 2009. Circulating oxidized low-density lipoprotein: A biomarker of atherosclerosis and cardiovascular risk? Clin Chem Lab Med 47:128–137.

Virmani R, Kolodgie FD, Burke AP, Finn AV, Gold HK, Tulenko TN, Wrenn SP, Narula J. 2005. Atherosclerotic plaque progression and vulnerability to rupture: Angiogenesis as a source of intraplaque hemorrhage. Arterioscler Thromb Vasc Biol 25:2054–2061.

Wang J, Chen S, Ma X, Cheng C, Xiao X, Chen J, Liu S, Zhao B, Chen Y. 2013. Effects of endothelial progenitor cell-derived microvesicles on hypoxia/reoxygenation-induced endothelial dysfunction and apoptosis. Oxid Med Cell Longev 2013:572729.

Yin KJ, Hamblin M, Chen YE. 2014. Non-coding RNAs in cerebral endothelial pathophysiology: Emerging roles in stroke. Neurochem Int 77C:9–16.

Zheng L, Xu CC, Chen WD, Shen WL, Ruan CC, Zhu LM, Zhu DL, Gao PJ. 2010. MicroRNA-155 regulates angiotensin II type 1 receptor expression and phenotypic differentiation in vascular adventitial fibroblasts. Biochem Biophys Res Commun 400:483–488.

Zhu LX, Liu J, Xie YH, Kong YY, Ye Y, Wang CL, Li GD, Wang Y. 2004. Expression of hepatitis C virus envelope protein 2 induces apoptosis in cultured mammalian cells. World J Gastroenterol 10:2972–2978.

Zhu N, Zhang D, Chen S, Liu X, Lin L, Huang X, Guo Z, Liu J, Wang Y, Yuan W, Qin Y. 2011. Endothelial enriched microRNAs regulate angiotensin II-induced endothelial inflammation and migration. Atherosclerosis 215:286–293.

SUPPORTING INFORMATION

Additional Supporting Information may be found in the online version of this article at the publisher's web-site.